Journal of Applied Polymer Science

Enhancement of mechanical and optical performance of commercial polystyrenes by blending with siloxane-based copolymers

Mario Daniel Ninago,[1] Vivina Hanazumi,[1] María Gabriela Passaretti,[1] Daniel Alberto Vega,[2] Andrés Eduardo Ciolino,[1] Marcelo Armando Villar[1]

[1]Departamento de Ingeniería Química, PlantaPiloto de Ingeniería Química, PLAPIQUI (UNS-CONICET), Universidad Nacional del Sur (UNS), Camino "La Carrindanga" Km 7, Bahía Blanca 8000, Argentina

[2]Departamento de Física, Instituto de Física del Sur—IFISUR, CONICET, Universidad Nacional del Sur (UNS), Av. Alem 1253, Bahía Blanca 8000, Argentina

Correspondence to: M. D. Ninago (E-mail: mninago@plapiqui.edu.ar)

ABSTRACT: Well-defined poly(styrene-*block*-dimethylsiloxane) copolymers (PS-*b*-PDMS) with low polydispersity index (M_w/M_n) and different compositions were synthesized by sequential anionic polymerization of styrene (S) and hexamethyl(ciclotrisiloxane) (D_3) monomers. Synthesized PS-*b*-PDMS copolymers were characterized by ^{1}H-nuclear magnetic resonance (^{1}H-NMR), size exclusion chromatography (SEC), Fourier transform infrared spectroscopy (FTIR), and transmission electron microscopy (TEM). The physicochemical characterization determined that block copolymers have molar mass values close to ~135,000 g mol^{-1}, narrow $M_w/M_n < 1.3$, and chemical composition ranging from low to intermediate PDMS content. Blends of these copolymers with a commercial polystyrene (PS) were obtained by melt mixing and subsequently injection. Films obtained were flexible, and showed lower transparency than the original PS matrix. On the other hand, a 10 wt % incorporation of PS-*b*-PDMS copolymers leads to better mechanical performance by enhancing elongation at break (~8.8 times higher) and opacity values (~18 times higher). In addition, UV–Vis barrier capacity of the resulting blends is also increased (up to 400% higher). © 2017 Wiley Periodicals, Inc. J. Appl. Polym. Sci. **2017**, *134*, 45122.

KEYWORDS: blends; copolymers; polystyrene; synthesis and processing techniques; thermoplastics

Received 19 December 2016; accepted 17 March 2017

DOI: 10.1002/app.45122

INTRODUCTION

Blending of two or more different polymers became an effective and inexpensive way to produce new materials with specific end uses and a wider range of properties. Nevertheless, the behavior of a multiphase polymer system cannot be univocally deduced from the properties of the individual phases because it depends on many factors, such as the spatial organization of each phase and the characteristics of the interface, among others.[1] Concerning to potential applications of polymer blends, optical properties of films is relevant since conditions future applications, especially for food packaging. In this sense, polymeric materials that are exposed to ultraviolet light (UV) might present chain breakage or oxidation of polymer units, which result in the reduction of thermal and mechanical properties leading to degraded structures.[2,3]

Traditionally, polyolefin blends used as packaging materials exhibited balanced mechanical and barrier properties.[4] Therefore, absorption and transmission of UV and visible light by polymers must be taken into account, especially for those applications in which products must be preserved or are sensitive to those wavelight radiations.[5,6] Thus, protecting biological systems and organic materials from UV radiation is a significant issue for engineering materials in both terrestrial and space applications.[2] In addition, optical properties, mainly color, transparency and UV absorption capacity are relevant issues since they conditioned the consumer acceptability of packed products.[7]

Polystyrene (PS) is a commodity polymer used in many fields, such as packaging of electrical equipment, apparatus, instruments, and food; as thermal insulation material for buildings; for cold storage purposes; and for disposable meal services.[8] PS has good optical and chemical properties that are employed for specific applications, such as aircraft glazing, signs, lighting, architecture, transportation, engineering, and high-performance products.[9] However, its highly brittle nature reduces applications requiring bendable, expandable, and/or cladding materials.[2] In this sense, the development of PS-based materials having flexibility, optical, and barrier properties would be of interest for certain applications.

Table I. Physicochemical Characterization of a Commercial PS Matrix and PS-*b*-PDMS Copolymers

Sample	S/D$_3$[a] (molar ratio)	Yield[b] (%)	M_n[c] (g/mol)	M_w/M_n[c]	x_{PDMS}[d]	w_{PDMS}[d]	T_{g1}[e] (°C)	T_{g2}[e] (°C)
PS	-	-	272,000	2.16	-	-	-	102.5
S$_{89}$DMS$_{11}$	5.8	96.7	138,000	1.29	0.28	0.11	-	102.5
S$_{78}$DMS$_{22}$	2.5	95.9	135,000	1.25	0.43	0.22	−125.6	102.6
S$_{45}$DMS$_{55}$	0.6	97.4	137,000	1.21	0.63	0.55	−125.1	102.1

[a] Styrene/dimethylsiloxane molar ratio.
[b] Percentage of reaction yield.
[c] Number average molar mass (M_n) and polydispersity indexes (M_w/M_n) determined according to SEC analysis.
[d] Molar (x_{PDMS}) and weight fraction (w_{PDMS}) calculated from ^{1}H-MNR spectra.
[e] Glass transition temperatures of PDMS and PS blocks (T_{g1}, T_{g2} respectively), determined by DSC.

Traditionally, mechanical properties of commercial PS can be enhanced through the dispersion of rubber particles into the PS matrix. These materials are usually produced by radical polymerization of the monomer in the presence of poly(butadiene), and the resulting polymer is known as high-impact polystyrene (HIPS). This methodology involves a complex synthesis in order to obtain grafted copolymers during the conventional polymerization of styrene. But besides this *in situ* polymerization, polymer blending is an alternative and an easy way to improve PS properties by using industrially available processing equipment.[10,11]

Poly(dimethylsiloxane) (PDMS) is a border line polymer between organic and inorganic materials which has been employed in a wide range of applications due to its unique features, such as excellent low temperature flexibility, low surface energy, and high thermal stability.[12] Consequently, PS/PDMS blends have been prepared for many purposes including the fabrication of membranes with hydrophobic surfaces; modification of rubbers; and production of specific materials for tribological applications.[13–15] However, stability problems arise from PS/PDMS blends mainly due to the migration of PDMS to the surface, as well as from its nonuniform dispersion in the PS matrix.[13,15]

A good dispersion of a given polymer into another polymeric matrix can be achieved by the addition of block copolymers. A block copolymer added to a blend of polymers acts as steric stabilizer because of miscibility among blocks and the corresponding homopolymers. Therefore, interfacial tension and average dimensions of domains are reduced.[16] Block copolymers constitute a group of materials belonging to the "soft matter" family, in which blocks from different polymeric chains are chemically bonded. In most cases, blocks are thermodynamically incompatible but the covalent bonds between them impose specific arrangements, by generating particular morphologies both in bulk and in solution. This behavior is a consequence of a microphase separation, induced by the thermodynamic incompatibility of the blocks.[14–24]

Taking into account the facts already discussed, in this work we propose the use of poly(styrene-*block*-dimethylsiloxane) copolymers (PS-*b*-PDMS) as an effective alternative to improve flexibility and final properties of a commercial PS matrix. PS/PS-*b*-PDMS blends were prepared by using 5 and 10 wt % of copolymers and by employing a melt mixing process. PS-*b*-PDMS copolymers were characterized by nuclear magnetic resonance (^{1}H-NMR), size exclusion chromatography (SEC), Fourier transform infrared spectroscopy (FTIR), and transmission electron microscopy (TEM) before mixing.

Films from the PS matrix and PS/PS-*b*-PDMS blends were obtained by thermocompression, and their thermal and mechanical behavior was evaluated by complementary characterization techniques, such as differential scanning calorimetry (DSC), thermogravimetric analysis (TGA), and tensile strength tests. In addition, opacity values and UV barrier capacity were studied. From these results, the effects of addition of PS-*b*-PDMS copolymers on final properties of the blends (compared to the original PS matrix) are displayed and discussed.

EXPERIMENTAL

Materials

Solvents and monomers employed in the synthesis of block copolymers were purified by standard anionic polymerization procedures reported in literature. These procedures provide solvents and monomers with a high-purity level. For further details, the reader is encouraged to refer to the excellent reviews from Hadjichristidis *et al.*,[25] Uhrig and Mays,[26] and many papers regarding this subject that can be found in the scientific literature.[25–29] Commercial *n*-buthyllithium solution (*n*-Bu$^-$Li$^+$, 1.6*M* in hexanes, Sigma Aldrich) was employed as anionic initiator. Styrene (S, Sigma Aldrich) and hexamethyl(cyclotrisiloxane) (D$_3$, Sigma Aldrich) were employed as monomers. Ciclohexane (Dorwill) and methanol (Química Industrial) were used as solvent and terminating agent, respectively. Tetrahydrofuran (THF, Ciccarelli) was added as solvating agent in order to promote D$_3$ polymerization according to previously reported procedures.[30]

A commercial crystal polystyrene (PS, LX HH103), provided by Unistar Company, was used as matrix for PS/PS-*b*-PDMS blends. LX HH103 exhibited a relatively high molar mass (see Table I), high viscosity, and a low value of melt flow index (0.18 g/min) determined according to D1238 ASTM guidelines.

Synthesis of PS-b-PDMS Copolymers. Polymerizations were carried out in a specially designed Schlenk-type reactor (Figure 1), following the methodology reported in previous works.[28,30,31] In this sense, the general procedure for the synthesis of PS-*b*-PDMS copolymers is briefly described as follows. The reactor was connected to the vacuum line by using the VLC connection, and **R$_1$** and **R$_2$** stopcocks were opened. Then, S monomer previously

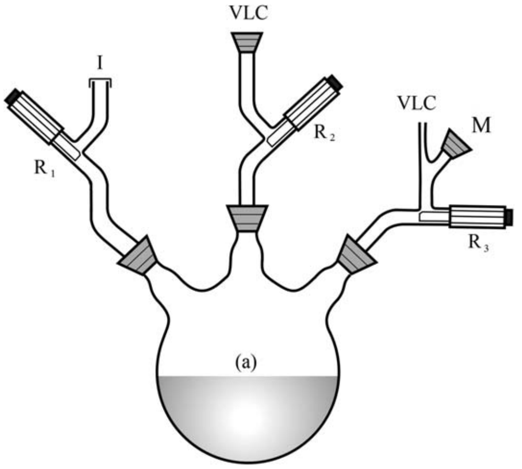

Figure 1. Schlenk-type reactor. References: (I) initiator, (M) styrene and hexamethylcyclotrilsiloxane monomers, (VLC) vacuum line connection, (R) stopcocks and (a) reactor.

collected in a vacuum flask was connected to the reactor by employing the **M** connection. After 2 min, the apparatus was flame dried and vacuum-pumped (20–30 min in order to remove volatile species inside). Subsequently, the reaction solvent (cyclohexane) was distilled from a collection flask already attached to the vacuum line. After two freezing-thawing cycles, S monomer was introduced into the reactor by opening the $\mathbf{R_3}$ stopcock. The monomer flask was detached, and S inside the reactor was thoroughly mixed with the solvent by employing gently hand movements. Thereafter, the required amount of commercial *n*-$Bu^{-}Li^{+}$ solution was injected (by using a syringe) through septum **I** by opening the $\mathbf{R_1}$ stopcock. The beginning of polymerization reaction was immediately evidenced by the typical color of poly(styril)lithium anions, $PS^{-}Li^{+}$ (bright orange). Polymerization was left to proceed at room temperature until all injected monomer was really consumed (usually, 24 h).[29,31]

An aliquot of the resulting PS was collected for subsequent characterization. After that, D_3 monomer already collected in an additional flask was added by opening the $\mathbf{R_3}$ stopcock, and the reaction was left to proceed at room temperature during ~20 h in order to favor the equilibration reaction between D_3 and $PS^{-}Li^{+}$. As it is reported in the literature, by this procedure the formation of $PS(CH_3)_2SiO^{-}Li^{+}$ species are obtained.[32] Finally, THF was added by opening the $\mathbf{R_3}$ stopcock to change the polarity of the reaction medium, promoting the polymerization of the remaining D_3. This final step was carried out at 50 °C, during 8 h.[29,33] The reaction was finished by injecting approximately 5 mL of methanol through septum **I**. Obtained block copolymers were precipitated in cold methanol, under magnetic stirring, dried under vacuum and kept stored in a dry place.

Characterization of PS-*b*-PDMS Copolymers

Size-Exclusion Chromatography (SEC). Samples were characterized by SEC on a system built with a Waters® 515 HPLC pump and a Waters® model 410 differential refractometer, equipped with three mixed bed PLGel linear columns and a precolumn with 5 μm bead size (PLGel). Elution solvent was toluene (Aldrich), flowing at a rate of 1 mL min^{-1} at room temperature. Injection volume was 200 μL, and PS standards were used for calibration. Mark-Houwink calibration constants used for PS were $K_{PS} = 0.012$ mL g^{-1}, $\alpha_{PS} = 0.71$.[34]

Nuclear Magnetic Resonance (^{1}H-NMR). ^{1}H-NMR spectra of PS-*b*-PDMS copolymers were recorded on a Bruker® 300 MHz instrument, using deuterated chloroform ($CDCl_3$, Aldrich) as solvent. About 5 to 10 mg of sample was diluted directly in the NMR tubes, at room temperature, by using an appropriate volume of solvent. Chemical composition of synthesized copolymers was obtained by using the values of integrated areas from characteristic ^{1}H signals of each block.

Codes

PS-*b*-PDMS copolymers were labeled as $S_{\#}DMS_{100-\#}$, in which # accounts for the wt % of PS block in the corresponding copolymer.

Transmission Electron Microscopy (TEM). Samples of block copolymers were dissolved in a nonselective solvent (toluene, 10 wt %). Films were prepared from this solution by casting one-drop, and by using water as substrate. The thin films so obtained were transferred to a copper grid and observed in a JEOL® 100 CXII apparatus, with 100 kV and 3 Å resolution.

Differential Scanning Calorimetry (DSC). Thermal properties of PS-*b*-PDMS copolymers were studied by using DSC, employing a Pyris 1 Perkin-Elmer® equipment. Samples were measured under He atmosphere, using approximately 10 mg of each of them, and heated from −140 °C to 200 °C. Then, they were kept at 200 °C during 5 min in order to eliminate the thermal history. After cooling at 10 °C min^{-1}, samples were heated again from −140 °C to 200 °C at a heating rate of 10 °C min^{-1}. From this second heating sequence, the glass transition temperature of PDMS (T_{g1}) and PS (T_{g2}) blocks were determined.

Preparation, Chemical Characterization, and Analysis of the Final Properties of Blends

Blends of Commercial PS with PS-b-PDS Copolymers. Polymer blends were obtained by melt mixing the commercial PS with 5 and 10 wt % of each copolymer. In all cases, 1.75 g or 3.5 g of the corresponding block copolymer was added to 33.25 g or 31.5 g of PS matrix placed in a beaker. By employing a spatula, materials were manually mixed and then were transferred to the Brabender Plastograph® chamber to promote melt mixing. Special care was taken in order to transfer quantitatively all materials. Mixtures were kept during 15 min at a nominal temperature of 200 °C under nitrogen atmosphere. Blends were prepared per batch, by using cam-blades at 50 rpm. The resulting material was removed from the mixer chamber and compressed between aluminum plates to obtain samples of approximately 3 mm thick. Table II summarizes names, formulations of the blends essayed, and weight fraction of poly(dimethylsiloxane) δ_{PDMS} on each PS/PS-*b*-PDMS blend.

Preparation of Films. Films of PS/PS-*b*-PDMS blends were prepared by thermocompression molding, using a hydraulic press at 180 kg cm^{-2}, at 200 °C, during 6 min of compression. The procedure employed assured obtaining homogeneous films suitable for subsequent analyses. Obtained films exhibited a thickness between 200 and 215 μm. These values were measured

Table II. Mechanical Properties of a Commercial PS Matrix and PS/PS-*b*-PDMS Blends

Sample	δ_{PDMS}[a]	Thickness[b] (μm)	σ[c] (MPa)	E[c] (MPa)	ε[c] (%)
PS	-	211.5 ± 8.7	30.8 ± 1.7	1,990 ± 177	2.19 ± 0.15
$(PS/S_{89}DMS_{11})_{5\%}$	0.005	203.9 ± 9.1	30.7 ± 2.1	2.199 ± 193	1.71 ± 0.66
$(PS/S_{78}DMS_{22})_{5\%}$	0.011	201.7 ± 9.7	30.1 ± 2.8	2,157 ± 141	2.15 ± 0.30
$(PS/S_{45}DMS_{55})_{5\%}$	0.023	205.1 ± 6.8	38.9 ± 2.6	2,820 ± 190	9.90 ± 0.85
$(PS/S_{89}DMS_{11})_{10\%}$	0.011	213.4 ± 7.6	30.3 ± 2.3	2,380 ± 185	2.30 ± 1.80
$(PS/S_{78}DMS_{22})_{10\%}$	0.022	215.4 ± 9.5	35.1 ± 3.1	2,490 ± 255	12.30 ± 0.96
$(PS/S_{45}DMS_{55})_{10\%}$	0.055	208.7 ± 8.7	45.1 ± 3.7	3,300 ± 280	19.29 ± 1.50

[a] Weigth fraction of poly(dimethylsiloxane) δ_{PDMS} in PS/PS-*b*-PDMS blends.
[b] Thickness measured by a micrometer.
[c] Maximum tensile strength (σ_{max}), elongation at break (ε %), and elastic modulus (*E*) calculated from stress–strain tests.

using a micrometer Mahr Millimar C 1208 (Mahr GmbH-Göttingen, Germany) and an inductive probe with an accuracy of 99.7%. Thickness variation among specimens of a given material was no larger than 10 μm.

Fourier Transform Infrared Spectroscopy (FTIR). Fourier transform infrared spectroscopy (FTIR) spectra of selected samples were obtained on a Nicolet® FTIR 520 spectrometer. Cast films from diluted solutions of the samples (1 wt % in THF) were obtained onto NaCl windows. FTIR spectra were recorded at 4 cm^{-1} resolution, over the 4,000–400 cm^{-1} range, by using an accumulation of 64 scans and dried air as background.

Thermogravimetric Analysis (TGA). Thermal degradation of samples was carried out in a TA Instrument® Discovery Series thermogravimetric balance. Samples were heated from 35 to 700 °C at 10 °C min^{-1} under nitrogen flow. Curves of weight loss versus temperature were recorded, and the maximum decomposition temperature was obtained from the corresponding first derivative curve.

Optical Properties. Opacity and UV barrier capacity were estimated from the absorbance spectrum (200–800 nm) recorded on a PG Instrument® T60 UV-Visible spectrophotometer. Films were cut into rectangles and placed on the internal side of a quartz cell. Film opacity (AU nm) was defined as the area under the curve (380–780 nm), according to ASTM D1003–00.[35,36] Film transparency was estimated by using a modified ASTM D1746–97 method, and according to the procedure already reported by Alvarado-González *et al.*[37]

Films color measurements were performed by using a Hunterlab® UltraScan XE colorimeter, in the transmittance mode. Color parameters *L*, *a*, and *b* were recorded according to the Hunter scale, in at least ten randomly selected positions for each film sample. Color parameters range from $L = 0$ (black) to $L = 100$ (white), $-a$ (greenness) to $+a$ (redness), and $-b$ (blueness) to $+b$ (yellowness). Standard values considered were those reported for white background ($L = 97.75$, $a = -0.49$, and $b = 1.96$). Corresponding values of ΔL, Δa, and Δb were calculated taking into account the standard values for white background, and the parameter color difference ΔE was determined by following eq. (1) proposed by Monedero *et al.*[38]

$$\Delta E = \sqrt{(\Delta a)^2 + (\Delta b)^2 + (\Delta L)^2} \tag{1}$$

Mechanical Properties. Mechanical properties of PS and PS/PS-*b*-PDMS blends prepared were determined by employing an Instron® 3369 universal machine, through tensile tests. For stress–strain tests, 10 probes of 13 × 100 mm were assayed. Maximum tensile strength (σ_{max}), elongation at break (ε %), and elastic modulus (*E*) were calculated according to the ASTM D882–00 guidelines.

Statistical Analysis. Analysis of variance (ANOVA) was used to compare mean differences between properties of PS matrix and PS/PS-*b*-PDMS blends. A comparison of mean values from UV/Vis, opacity and mechanical properties of the essayed samples was performed by Fisher's least significant difference test, conducted at a significance level $P = 0.05$.

RESULTS AND DISCUSSION

Synthesis and Chemical Characterization of PS-*b*-PDMS Copolymers

PS-*b*-PDMS copolymers were synthesized by employing anionic polymerization and sequential addition of monomers, in a Schlenk-type reactor (Figure 1) by following the classical methodology reported in the literature.[25,28] For such a purpose, two main objectives were imposed: (i) a proper purification of monomers and reagents; and (ii) the precise methodology for controlling D_3 polymerization.[26,30,39] By following these objectives, three different PS-*b*-PDMS copolymers were synthesized. Table I summarizes the names assigned, the values of monomers molar ratios (styrene/dimethylsiloxane), the yield obtained, and the molecular characterization. PS-*b*-PDMS copolymers showed molar masses at around 137,000 g mol^{-1} and different siloxane contents. In addition, their polydisperisity index (M_w/M_n) are lower than 1.3. The reason why M_w/M_n is higher than conventional anionic polymerization (high vacuum techniques)[28–30,33] can be explained by taking into account that the experimental procedure employed in this work involves only a vacuum manifold (no purified nitrogen or argon gas was employed), and the closing and opening of vacuum stopcocks (Rotaflo®) from different devices that are attached and de-attached from the main reactor. These manipulations might contaminate, in some extent, the vacuum by introducing air inside the reactor. Consequently, the "clean" medium might be lost and the overall

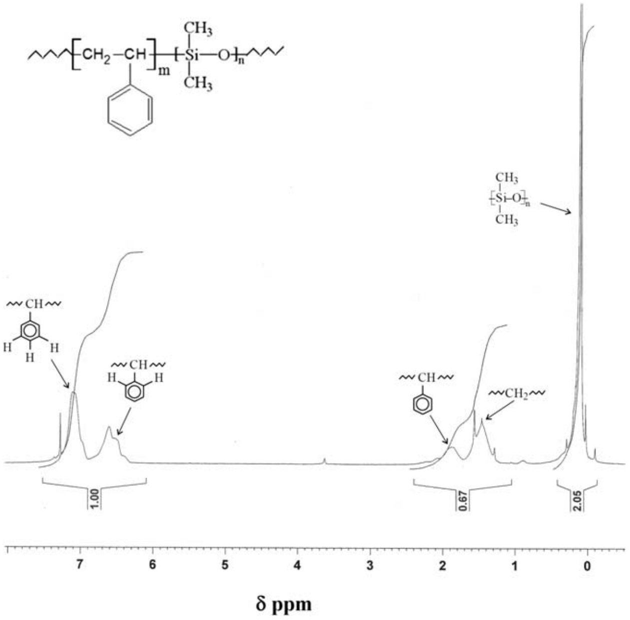

Figure 2. ^{1}H-NMR spectrum of $S_{45}DMS_{55}$ copolymer.

synthesis will result in broader M_w/M_n values. Although the procedure involves some loss of control over M_w/M_n, its simplicity to obtain the desired polymers with quite acceptable control might favor its application.

Molar and weight fraction of PDMS in the copolymers (x_{PDMS} and w_{PDMS}) were determined by ^{1}H-NMR considering the ^{1}H from methyl groups directly bonded to silicon atoms ($((C\mathbf{H_3})_2SiO^-)$) at $\delta = 0.14$ ppm, and the ^{1}H from the aromatic rings of styrene units ($C_6\mathbf{H_5}$-CH-CH_2-) between $\delta = 6.1$ ppm and 7.6 ppm.[28,29,40] A typical ^{1}H-NMR spectrum of copolymers is shown in Figure 2.

Thermal properties of PS-*b*-PDMS copolymers were studied by DSC. Glass transition temperature of PDMS ($T_{g1} \sim -125\,°C$) and PS ($T_{g2} \sim 102\,°C$) were determined (Table I). Obtained values are in accordance with those reported in the literature for these copolymers.[41] PS-*b*-PDMS block copolymers are really stable since both blocks are stable. Thermal stability of these copolymers has been reported, and there is no evidence of intra or inter blocks breaking. Moreover, the absence of reactive groups close to C-Si bond prevents block splitting.[42,43]

In order to check morphological feature with the results obtained by ^{1}H-NMR, PS-*b*-PDMS copolymers were studied by TEM. As examples, Figure 3 shows TEM micrographs patterns formations of $S_{89}DMS_{11}$ and $S_{45}DMS_{55}$ copolymers. For the copolymer with the lower w_{PDMS} value [$S_{89}DMS_{11}$, Figure 3(a)], a microphase separation is developed in which the dark PDMS pseudo-spheres can be distinguish among the white regions associated to PS. According to Wu *et al.*,[22] and Sawyer and Drubb,[44] PS-*b*-PDMS copolymers showed microphase separation in which the dark and white regions represent the domains of PDMS and PS, respectively. This effect could be associated with the higher scatter ability of the Si atoms compared to C atoms,[22,44] as well as differences in the solubility parameter of each segment.[42] Also, for the $S_{45}DMS_{55}$ copolymer [Figure 3(b)] a kind of rod-like microphase separation can be appreciated. According to previous works,[45] cast films of PS-*b*-PDMS from toluene solutions give a “spaghetti-like” structure because toluene is a good solvent for both blocks. This structure is considered as an hybrid between rod and sphere structures due to the high interfacial contact energy between blocks. Consequently, the reactive area is enhanced.

Characterization of PS/PS-*b*-PDMS Blends

Figure 4 shows the FTIR spectra of PS matrix and PS/$S_{78}DMS_{22}$ blend. Arrows indicate common bands, and the most significant resemblances between spectra will be described as follows. PS spectrum shows an absorption band at 3026 cm^{-1} (Ref. 22) associated to the vibration of -HC=CH- bonds from aromatic rings and a vibration corresponding to –CH_2– groups at 2860 cm^{-1} (Ref. 46). At 1600 cm^{-1} (Ref. 47) was observed the absorption band attributed to C=C bonds; and finally, at 908 cm^{-1} (Refs. 47 and [48]) the absorption band corresponding to mono substituted aromatic compounds was detected. For the PS/$S_{78}DMS_{22}$ blend, despite the absorption bands already assigned to the PS matrix (that will resemble those at PS block), typical absorptions bands corresponding to PDMS block can be recognized in the spectrum. At 2963 cm^{-1} appears the absorption band corresponding to C–H bonds from -CH_3 groups attached to Si atoms.[49] The out of phase vibrations of Si–$(CH_3)_2$ and O–Si–OR bonds appear at 1260 cm^{-1} (Ref. 50); and finally, at 1093 cm^{-1} (Ref. 32) appears the absorption band corresponding to the symmetric vibration of Si–O–Si bonds.[46] In addition, the absorption band corresponding to the C–Si–C bonds is clearly observed at 1024 cm^{-1} (Refs. 48–50).

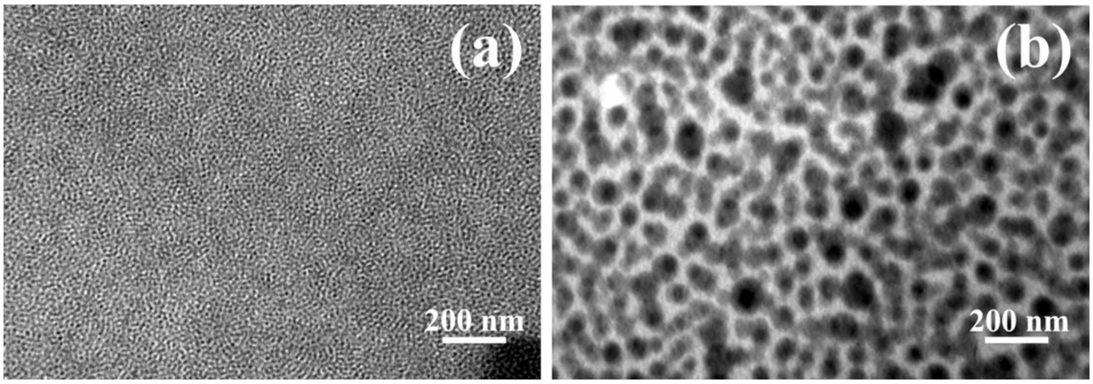

Figure 3. TEM images: (a) $S_{89}DMS_{11}$ copolymer (100,000×); and (b) $S_{45}DMS_{55}$ copolymer (100,000×).

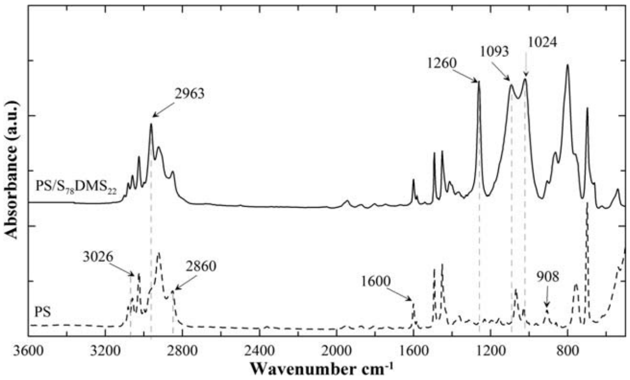

Figure 4. FTIR spectra of a commercial PS and a PS/$S_{78}DMS_{22}$ blend.

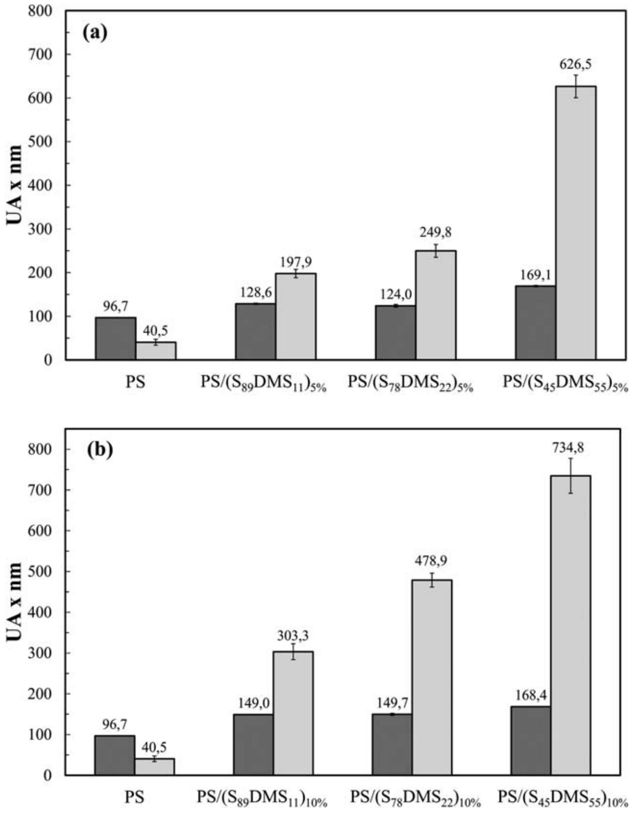

Figure 6. UV barrier capacity values of the PS matrix and blends with (a) 5 wt % and (b) 10 wt % of block copolymers. Symbols: (■) absorption, (□) opacity.

Thermogravimetric measurements were used to evaluate degradation processes of commercial PS and PS/PS-*b*-PDMS blends. Figure 5 shows the TGA and the first derivative curves for commercial PS matrix and for blends with the highest copolymer content (10 wt %). As it can be observed, commercial PS shows a weight-loss step at ~425 °C [Figure 5(a)], in agreement with data published by Adnan and Jan.[51] On the other hand, the weight-loss step for PDMS is observed in the 510 to 590 °C range, which could be attributed to oxidation reactions of PDMS bonds.[35] As it can be appreciated in Figure 5(b), blends with the higher PDMS content (labeled as $(PS/S_{78}DMS_{22})_{10\%}$ and $(PS/S_{45}DMS_{55})_{10\%}$, respectively) present the typical thermal degradation events associated to both, PS and PDMS homopolymers. As conclusion, it can be pointed out that 5 and 10 wt % of PS-*b*-PDMS in blends would not compromise the thermal stability of PS matrix.

Final Properties of Prepared Blends

Figure 6 shows UV–Vis data obtained from selected films. As it can be observed, values indicate that blends show higher opacity when compared to commercial PS matrix. In this sense, the opacity value for the $(PS/S_{45}DMS_{55})_{5\%}$ was ~15 times higher than the value obtained for PS matrix [Figure 6(a)]. Similarly, for the $(PS/S_{45}DMS_{55})_{10\%}$ blend, the opacity value was increased ~18 times [Figure 6(b)]. Additionally, blends PS/$S_{89}DMS_{11}$ and PS/$S_{78}DMS_{22}$ also showed an increase in opacity values, but in less proportion. These noticeable increments in

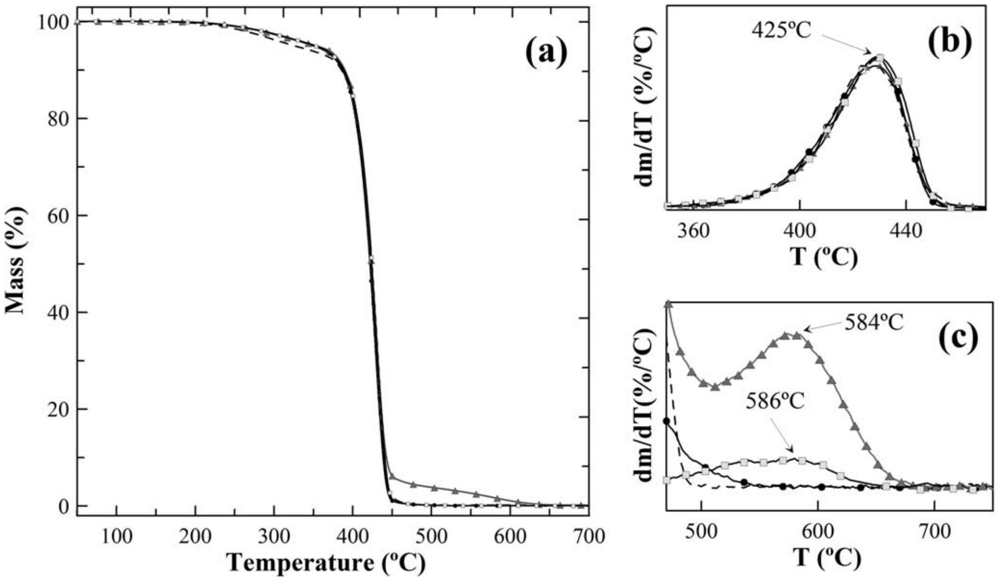

Figure 5. Weight loss (a) and first derivative (b, c) TGA curves for commercial PS and blends with 10 wt % of block copolymers. Symbols: (—) PS, (●) $(PS/S_{89}DMS_{11})_{10\%}$, (□) $(PS/S_{78}DMS_{22})_{10\%}$, (▲) $(PS/S_{45}DMS_{55})_{10\%}$.

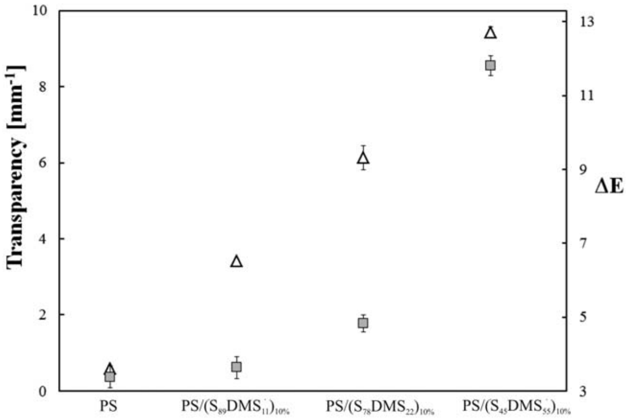

Sample	L	*a*	*b*	ΔE	Transparency [#]
PS	94.34±0.03	-0.16±0.01	-0.48±0.04	3.03±0.28	0.58±0.07
(PS/S$_{89}$DMS$_{11}$)$_{5\%}$	95.54±0.07	0.15±0.01	-0.29±0.01	3.23±0.10	2.61±0.03
(PS/S$_{78}$DMS$_{22}$)$_{5\%}$	94.40±0.27	0.51±0.04	0.98±0.08	4.20±0.30	4.31±0.31
(PS/S$_{45}$DMS$_{55}$)$_{5\%}$	90.72±0.18	0.79±0.03	2.82±0.11	7.24±0.19	7.61±0.15
(PS/S$_{89}$DMS$_{11}$)$_{10\%}$	95.72±0.10	0.13±0.02	-0.61±0.02	3.33±0.28	3.42±0.24
(PS/S$_{78}$DMS$_{22}$)$_{10\%}$	93.50±0.33	0.47±0.12	1.05±0.14	4.52±0.23	6.13±0.23
(PS/S$_{45}$DMS$_{55}$)$_{10\%}$	86.45±0.26	0.78±0.03	3.89±0.11	11.53±0.27	9.42±0.52

Hunter color parameters: Luminosity (*L*), -*a* (greenness) to +*a* (redness), -*b* (blueness) to +*b* (yellowness) and parameter color difference (ΔE). [#] Transparency determined by UV-vis spectrometer

Figure 7. Colorimetric measurements for a commercial PS matrix and PS/PS-*b*-PDMS blends. Symbols: (Δ) transparency, (□) ΔE.

opacity values could be associated with the increasing size of PDMS block in the copolymers, which could scatter light and lead to higher opacity values. Besides, the presence and size of siloxane segment into the block copolymers, lead to macrophase separations of domains into PS/PS-*b*-PDMS blends.[4,13,47] In this sense, Chen *et al.*[35] reported a similar behavior studying optical properties of PDMS composites reinforced with silicone.

Regarding the UV barrier capacity, it is important to highlight that commercial PS presented the ability to absorb UV radiation, since a peak in the 270 to 300 nm range was found in the UV–Vis spectra (Figure 6). The incorporation of 5 and 10 wt % of block copolymers enhanced absorption values. A similar increment in the UV barrier capacity by the incorporation of 5% and 10 wt % of the S$_{45}$DMS$_{55}$ block copolymer was observed [Figure 6(a,b)]. In this sense, for (PS/S$_{45}$DMS$_{55}$)$_{10\%}$, obtained values resulted ~400% higher compared to PS matrix. These results can be compared to those obtained by Jairam *et al.*,[2] which reported an equivalent behavior for composites of PS/butyl acrylate, where the composites presented light UV-blocking capacity. Regarding transparency, Eita *et al.*[52] reported the use of PDMS in poly(methylmetacrylate) films as an alternative for developing a transparent UV-blocking material.

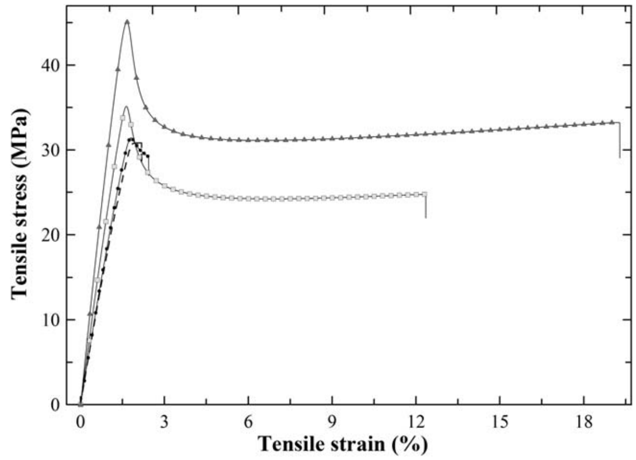

Figure 8. Tensile tests for a commercial PS and PS/PS-*b*-PDMS blends (10 wt %). Symbols: (—) PS, (●) (PS/S$_{89}$DMS$_{11}$)$_{10\%}$, (□) (PS/S$_{78}$DMS$_{22}$)$_{10\%}$,(▲) (PS/S$_{45}$DMS$_{55}$)$_{10\%}$.

Other relevant characteristic of the films obtained in the present work is their color attributes. Luminosity (*L*), chromaticity (*a*, *b*) and transparency values are shown in Figure 7. The incorporation of PS-*b*-PDMS copolymers modifies the L value of the commercial PS, as well as its chromaticity parameters (*a* and *b*) and transparency. According to Figure 7, the incorporation of PS-*b*-PDMS in the blends results in a decrease of the transparency due to an increase in the absorption at 600 nm. As it can be seen, the *L* values decreases up to ~10% by the incorporation of 5 and 10 wt % of S$_{45}$DMS$_{55}$ copolymer. However, at the same concentration, the incorporation of S$_{89}$DMS$_{11}$ and S$_{78}$DMS$_{22}$ copolymers showed almost no modification. Chromaticity values (*a*, *b*) were increased significantly, especially for blends with 10 wt % of S$_{45}$DMS$_{55}$ giving the films a yellowish greenish hue. The decreasing transparency of these blends could be attributed to the increasing molar fraction of PDMS in the block copolymer and consequently in the final blend (see Table II), as verified by TEM, which could scatter light and lead to opacity as shown before. The increment of the three parameters (*L*, *a*, and *b*) are reflected in an increase on the parameter color differences (Δ*E*).

Figure 8 shows tensile test curves corresponding to commercial PS and blends containing 10 wt% of block copolymers.

Mechanical properties obtained from tensile tests are summarized in Table II. The reinforcing effect of PS-*b*-PDMS copolymers to the commercial PS matrix is evident, according to elongation at break (ε %) and Young's modulus values (ε % and *E*, respectively). For (PS/S$_{89}$DMS$_{11}$)$_{5\%}$, and (PS/S$_{78}$DMS$_{22}$)$_{5\%}$ blends σ_{max} and ε % did not show significant changes compared to the PS matrix, and this effect could be associated with the low PDMS content in the copolymers. However, a slightly increment in *E* values is observed in all cases. In this sense, (PS/S$_{45}$DMS$_{55}$)$_{5\%}$, (PS/S$_{78}$DMS$_{22}$)$_{10\%}$, and (PS/S$_{45}$DMS$_{55}$)$_{10\%}$, blends exhibited σ_{max} values of ~1.1, ~1.3, and ~1.5 times higher than those corresponding to PS matrix, and *E* values were 1.2, 1.4, and 1.7 times higher. Finally, maximum ε % values are observed for (PS/S$_{45}$DMS$_{55}$)$_{5\%}$, (PS/S$_{78}$DMS$_{22}$)$_{10\%}$, and (PS/S$_{45}$DMS$_{55}$)$_{10\%}$ blends which resulted in 4.5, 5.6, and 8.8 times higher compared to the PS matrix.

From these results, it is clear that the incorporation of a styrene/dimethylsiloxane block copolymer as a second phase into a PS matrix has the advantage of combining interfacial adhesion by affinity, which results in a better compatibility between copolymer and PS matrix.[7,50] The PDMS block acts as rubbery-like material, so its influence over a PS matrix can be thought similar to natural rubber or polybutadiene. It is well known that the addition of rubbery materials onto PS matrices exerts a marked influence on the final properties of the resulting material,[53–55] and depending on the particle size and experimental conditions[56] diminishes the brittle behavior of the PS matrix by enhancing its elongation at break and tensile stress. PS-*b*-PDMS copolymers offer a better alternative since the presence of PS block enhances the compatibility with the matrix and their influence over the mechanical properties of the resulting blend might be independent of particle size and mixing conditions. Although this is not quite true, siloxane-based copolymers enhance the final properties of PS matrices (surface and mechanical properties), especially if they are block-type copolymers.[56–58] By comparing this alternative to *in situ* polymerization, polymer blending is an easy way to obtain improved PS-based materials, which can be produced by using the processing equipment commonly available in most industries. It is believed that by tuning the molecular structure of PS-*b*-PDMS copolymers particular characteristics for the PS matrix might be achieved, especially if the enhancements of UV/Vis barrier, opacity or mechanical properties are expected.

CONCLUSIONS

PS-*b*-PDMS copolymers were used as reinforcing material in a commercial PS matrix. The copolymers were successfully synthesized by employing anionic polymerization (vacuum techniques) and sequential addition of monomers. Copolymers exhibited low polydispersity index ($M_w/M_n < 1.3$) and microphase separation, according to SEC and TEM analysis. Blends of PS-*b*-PDMS copolymers with commercial PS were suitably processed by melt mixing, and subsequently injected. According to TGA analysis, resulting blends were thermally stable, and the presence of block copolymers does not compromise the thermal stability of PS matrix. The blocking effect to visible, transparency and to UV radiations was evident for the blends obtained, since higher opacity (~18 times higher) and UV-barrier capacities (>400%) were observed. Finally, the incorporation of PS-*b*-PDMS copolymers into a PS matrix led to a better mechanical performance by increasing σ_{max} and ε % values in the resulting blends.

ACKNOWLEDGMENTS

We express our gratitude to the Consejo Nacional de Investigaciones Científicas y Técnicas de la República Argentina (CONICET, thanks to the PIP0428 Grant) and the Universidad Nacional del Sur (UNS, Argentina, PGI 24/M135 Grant) for their financial support.

REFERENCES

1. Gopi, J. A.; Nando, G. B. *Adv. Polym. Sci. Technol.* **2014**, *4*, 43.
2. Jairam, S.; Bucklin, R.; Correll, M.; Sakthivel, T. S.; Seal, S.; Truett, J.; Tong, Z. *Mater. Des.* **2016**, *90*, 151.
3. Joshi, G. V.; Pawar, R. R.; Kevadiya, B. D.; Bajaj, H. C. *Microporous Mesoporous Mater.* **2011**, *142*, 542.
4. Fortelný, I.; Šlouf, M.; Sikora, A.; Hlavatá, D.; Hašová, V.; Mikešová, J.; Jacob, C. *J. Appl. Polym. Sci.* **2006**, *100*, 2803.
5. Kuo, W. K.; Weng, H. P.; Hsu, J. J.; Yu, H. H. *Mater. Chem. Phys.* **2016**, *173*, 285.
6. Park, D. H.; Hong, J.; Park, I. S.; Lee, C. W.; Kim, J. K. *Adv. Funct. Mater.* **2014**, *24*, 5186.
7. López, O. V.; Castillo, L. A.; Barbosa, S. E.; Villar, M. A.; García, M. A. *Polym. Compos.* **2016**, DOI: 10.1002/pc.24073.
8. Çekingen, S. K.; Saltan, F.; Yildirim, Y.; Akat, H. *Thermochim. Acta* **2012**, *546*, 87.
9. Liu, K.; Kuang, C.; Zhong, M.; Shi, Y.; Chen, F. *Opt. Mater.* **2013**, *35*, 2710.
10. Guo, C.; Zhou, L.; Lv, J. *Polym. Polym. Compos.* **2103**, *21*, 449.
11. Magalhlest, A. M. L.; Borggreve, R. J. M. *Macromolecules* **1995**, *28*, 5841.
12. Gopi, J. A.; Nando, G. B. *Int. J. Plast. Technol.* **2015**, *19*, 288.
13. Busche, B. J.; Tonelli, A. E.; Balik, C. M. *Polymer* **2010**, *51*, 454.
14. Maric, M.; Macosko, C. W. *J. Polym. Sci. Part B: Polym. Phys.* **2002**, *40*, 346.
15. Chuai, C.; Li, S.; Almdal, K.; Alstrup, J.; Lyngaae-jørgensen, J. *J. Appl. Polym. Sci.* **2004**, *92*, 2747.
16. Lyngaae-Jørgensen, J. *Int. Polym. Proc.* **1999**, *XIV*, 213.
17. Ninago, M. D.; De Freitas, A. G. O.; Hanazumi, V.; Muraro, P. I. R.; Schmidt, V.; Giacomelli, C.; Ciolino, A. E.; Villar, A. M. *Macromol. Chem. Phys.* **2015**, *216*, 2331.
18. Ninago, M. D.; Satti, A. J.; Gómez, R. L.; Vega, D. A.; Ciolino, A. E.; Villar, M. A.; Vega, D. A. In Block Copolym. Phase Morphol. Mater. Appl. Future Challenges, Ryan H. Diaz, R. R.; Ferguson, A. P., eds.; Nova Science Publishers: New York, **2014**; p 1, Chapter 1.
19. Qin, X.; Li, Y.; Zhou, F.; Ren, L.; Zhao, Y.; Yuan, X. *Appl. Surf. Sci.* **2015**, *28*, 183.
20. Rasappa, S.; Schulte, L.; Borah, D.; Morris, M. A.; Ndoni, S. *Colloids and Interface Sci. Commun.* **2014**, *2*, 1.
21. Uhrig, D.; Mays, J. *Polym. Chem.* **2011**, *2*, 69.
22. Wu, N.; Huang, L.; Zheng, A. *Front. Chem. China* **2006**, *1*, 350.
23. Yuan, W.; Yuan, J.; Zhang, F.; Xie, X.; Pan, C. *Macromolecules* **2007**, *40*, 9094.
24. Toledo Hijo, A. A. C.; da Costa, J. M. G.; Silva, E. K. V.; Azevedo, M.; Yoshida, M. I.; Borges, S. V. *J. Food Process Eng.* **2015**, *38*, 1.
25. Hadjichristidis, M. P. N.; Iatrou, H.; Pispas, S. *J. Polym. Sci. Part A: Polym. Chem.* **2000**, *38*, 3211.
26. Uhrig, D.; Mays, J. W. *J. Polym. Sci. Part A: Polym. Chem.* **2005**, *43*, 6179.
27. Bellas, V.; Iatrou, H.; Hadjichristidis, N. *Macromolecules* **2000**, *33*, 6993.
28. Ninago, M. D.; Satti, A. J.; Ciolino, A. E.; Valles, E. M.; Villar, M. A.; Vega, D. A.; Sanz, A.; Nogales, A.; Rueda, D. R. *J. Polym. Sci. Part A: Polym. Chem.* **2010**, *46*, 3119.
29. Ninago, M. D.; Ciolino, A. E.; Villar, M. A.; Giacomelli, F. C.; Cernoch, P.; Stepánek, P.; Schmidt, v.; Giacomelli, C. *Chem. Eng. Trans.* **2009**, *17*, 1807.

30. Ninago, M. D.; Satti, A. J.; Ressia, J. A.; Ciolino, A. E.; Vallés, E. M.; Villar, M. A. *Chem. Eng. Trans.* **2009**, *17*, 1729.
31. Christodoulou, S.; Iatrou, H.; Lohse, D. J.; Hadjichristidis, N. *J. Polym. Sci. Part A: Polym. Chem.* **2005**, *43*, 4030.
32. Zundel, T.; Teyssié, F.; Jérôme, R. *Macromolecules* **1998**, *31*, 2433.
33. Gómez, L. R.; Vega, D. A.; Ninago, M. D.; Ciolino, A. E.; Villar, M. A.; Vallés, M. E. *Polymer* **2015**, *59*, 180.
34. Kurata, Y. T. M. In Polymer Handbook, 4th ed.; Grulke, E. A., Brandup, J., Immergut, E. H. Eds.; Wiley: New York, **1999**.
35. Chen, D.; Chen, F.; Hu, X.; Zhang, H.; Yin, X.; Zhou, Y. *Compos. Sci. Technol.* **2015**, *117*, 307.
36. Ninago, M. D.; López, O. V.; Lencina, M. M. S.; García, M. A.; Andreucetti, N. A.; Ciolino, A. E.; Villar, M. A. *Carbohydr. Polym.* **2015**, *134*, 205.
37. Alvarado-González, J. S.; Chanona-Pérez, J. J.; Welti-Chanes, J. S.; Calderón-Domínguez, G.; Arzate-Vázquez, I.; Pacheco-Alcalá, S. U.; Garibay-Febles, V.; Gutiérrez-López, G. F. *Rev. Mex. Ing. Química* **2012**, *11*, 193.
38. Monedero, F. M.; Fabra, M. J.; Talens, P.; Chiralt, A. *J. Food Eng.* **2009**, *91*, 509.
39. Zilliox, S. B. J. G.; Roovers, J. E. L. *Macromolecules* **1975**, *8*, 573.
40. Giacomelli, F. C.; Riegel, I. C.; Stepánek, P.; Petzhold, C. L.; Ninago, M. D.; Satti, A. J.; Ciolino, A. E.; Villar, M. A.; Schimidt, V.; Giacomelli, C. *Langmuir* **2010**, *26*, 14494.
41. Ciolino, A.; Sakellariou, G.; Pantazis, D.; Villar, M. A.; Vallés, E.; Hadjichristidis, N. *J. Polym. Sci. Part A: Polym. Chem.* **2006**, *44*, 1579.
42. Jiang, Y.; Shi, H.; Cai, M.; Liang, Y.; Li, B.; Zhang, H.; Song, R. *J. Appl. Polym. Sci.* **2013**, *129*, 247.
43. Lee, W.; Gil, S. C.; Lee, H.; Kim, H. al. *Macromol. Res.* **2009**, *17*, 451.
44. Sawyer, D. T.; Drubb, L. C. Polymer Microscopy, 2nd ed.; Wiley-VCH: London, **1996**.
45. Saam, J. C.; Fearon, F. W. G. *Ind. Eng. Chem. Prod. Res. Dev.* **1971**, *10*, 10.
46. Ninago, M. D.; Satti, A. J.; Ciolino, A. E.; Villar, M. A. *J. Therm. Anal. Calorimetry* **2013**, *112*, 1277.
47. Alkan, C.; Sarı, A.; Bicer, A. *J. Appl. Polym. Sci.* **2012**, *125*, 3447.
48. Dogan, F.; Kaya, I.; Dayan, O.; Özdemir, E. *J. Appl. Polym. Sci.* **2007**, *106*, 3454.
49. Liang, L.; Ruckenstein, E. *J. Membr. Sci.* **1995**, *114*, 227.
50. Agudelo, N. A.; Perez, L. D. *Mater. Res.* **2016**, *19*, 459.
51. Adnan, J. S.; Jan, M. R. *J. Anal. Appl. Pyrolysis* **2014**, *109*, 196.
52. Eita, M.; Sayed, R. E l.; Muhammed, M. *J. Colloid Interface Sci.* **2012**, *387*, 135.
53. Hobbs, S. Y. *Polym. Eng. Sci.* **1986**, *26*, 74.
54. Asaletha, R.; Kumarana, M. G.; Thomas, S. *Eur. Polym. J.* **1999**, *35*, 253.
55. Mathew, A. P.; Packirisamy, S.; Thomas, S. *J. Appl. Polym. Sci.* **2000**, *78*, 2327.
56. Lee, H.; Archer, L. A. *Macromol*ecules **2001**, *34*, 4572.
57. Wu, L.; Huang, L.; Zheng, A.; Xiao, H. *J. Appl. Polym. Sci.* **2006**, *99*, 2936.
58. Fayt, R.; Jérome, R.; Teyssié, P. H. *J. Polym. Sci. Part B: Polym. Phys.* **1989**, *27*, 775.